*Int. J. Heat Mass Transfer.* Vol. 30, No. 1, pp. 125–136, 1987
Printed in Great Britain

0017–9310/87 $3.00 + 0.00
Pergamon Journals Ltd.

# Analysis of the convective evaporation of nondilute clusters of drops

J. BELLAN and K. HARSTAD
Jet Propulsion Laboratory, California Institute of Technology,
4800 Oak Grove Drive, Pasadena, CA 91109, U.S.A.

(*Received* 9 *October* 1985 *and in final form* 1 *April* 1986)

**Abstract**—A model for the convective evaporation of nondilute clusters of drops has been developed. The critical parameter which controls the different evaporation modes has been identified to be the penetration distance of the outer flow into the cluster volume. A dynamic criterion has been developed to differentiate between penetration and no penetration. Convective evaporation was modeled using a Reynolds number correlation between the evaporation rate with and without convection. Other equations, previously developed [*Combust. Flame* **51**, 55–67 (1983)] for quiescent, nondilute-spray evaporation, have been used here as well, with the exception of a new kinetic-evaporation law at the droplet surface and a nonuniform interior temperature model which have both been developed here.

The model is shown to perform well for low penetration distances which are obtained for dense clusters in hot environments and low relative velocities between outer gases and cluster. For dense clusters with low penetration distances the results of the model predict that for the same initial velocity the evaporation time is shorter as the cluster becomes more dilute. For dilute clusters and large penetration distances, the opposite was found. Since for large penetration distances the predictive ability of the model deteriorates, these last trends are questionable. Furthermore, the evaporation time was found to be a weak function of the initial relative velocity and a strong function of the initial drop temperature. The initial surrounding gas temperature was found to have a strong influence in the lower temperature regime, 750–1500 K, whereas in the higher temperature regime the influence was very weak. The vitiation of the ambient gas by fuel vapor was found to have a very small influence upon the evaporation time for rich mixtures when the cluster is introduced in a strongly convective, high temperature surroundings. In all cases the results show that the interior drop-temperature was transient throughout the drop lifetime, but nonuniformities in the temperature persisted up to at most the first third of the total evaporation time.

## 1. INTRODUCTION

THE BEHAVIOR of sprays injected into combustors is of great practical interest because of the variety of power systems using liquid fuel as a source of energy. Typically, the liquid fuel is atomized into droplets in a chamber where it mixes with ambient gases and burns. The interaction between the spray and the ambient gas is complex due to turbulent effects which distort the shape of the spray as it moves through the chamber and disperse the droplets. Moreover, the proximity of the droplets in the spray leads to interactions between the drops themselves such as collisions, coalescence, hydrodynamic interactions and limitations on the evaporation rate due to local fuel vapor accumulation. The coupling of all these phenomena yields an extremely complicated physical picture that cannot presently be described by a model that is computationally reasonable. For this reason, the entire problem has traditionally been divided into simpler problems that are tractable and that usually emphasize a particular aspect of the physical situation with the aim of gaining a deeper understanding about it. The ultimate goal is to be able to use this understanding for the description of the more complicated problem.

In this paper, interest is focused on the nondilute aspect of sprays, and in particular on how it can influence droplet heating and evaporation in a convective flow. An issue that will be addressed here is, for example, that of the difference in the convective evaporation between a drop, a dilute spray and a dense spray for a given initial relative velocity. Moreover, for a given spray with a specified drop-number density, the question of the influence of the initial relative velocity between the gas and the spray will be considered. This is because it is important to know first how much of a reduction in the evaporation time can be expected by increasing the relative velocity and also to know if asymptotic behavior might be reached in the process. Further, the effects of the initial temperature of the surroundings and the initial temperature of the drops will be investigated. Finally, it will be shown that the initial vitiation by fuel vapor of the gas surrounding the spray has a negligible effect for rich mixtures, when the spray is introduced into a strongly convective, high-temperature surrounding gas.

Section 2 presents the model formulation while some equations previously developed are recalled in the Appendix. The numerical procedure used to solve the model equations is briefly outlined in Section 3.

## NOMENCLATURE

$a$ radius of the sphere of influence [cm]
$C$ nondimensional evaporation rate, $-\dot{m}/(4\pi\rho_g D R^\circ)$
$C_D$ drag coefficient
$C^*$ defined by equation (17)
$C_p$ heat capacity at constant pressure [cal g$^{-1}$ K$^{-1}$]
$D$ diffusivity [cm$^2$ s$^{-1}$]
$d_c$ effective cluster diameter [cm]
$f(R_1, R_2)$ $(R_2^3 - R_1^3)/3$
$g(R_1, R_2)$ $(e^{C/R_1} - e^{C/R_2})$
$I(R_1, R_2, C)$ $\int_{R_1}^{R_2} e^{C/y} y^2 \, dy$
$L$ latent heat of evaporation [cal g$^{-1}$]
$\dot{M}$ evaporation flux [g cm$^{-2}$ s$^{-1}$]
$m$ mass [g]
$\dot{m}$ evaporation rate [g s$^{-1}$]
$N$ total number of drops
$n$ density of drops in the cluster [cm$^{-3}$]
$p$ pressure [atm]
$R$ radius of a drop [cm]
$\hat{R}_u$ universal gas constant [atm$^2$ s$^2$ cm$^4$ g$^{-1}$ mol$^{-1}$ K$^{-1}$]
$R_u$ universal gas constant [cal mol$^{-1}$ K$^{-1}$]
$R^*$ defined by equation (20)
$R_u^*$ universal gas constant [atm cm$^3$ mol$^{-1}$ K$^{-1}$]
$\tilde{R}_u$ cluster radius [cm]
$R_1$ $R/R^\circ$
$R_2$ $a/R^\circ$
$r$ radial coordinate [cm]
$\mathscr{S}$ $4\pi\tilde{R}^2$ [cm$^2$]
$T$ temperature [K]
$\hat{T}^1$ $\int_1^{R_2} [\theta_g^\circ(y) - 1] y^2 \, dy + \hat{V}_1(\theta_{ga}^\circ - 1)$
$\hat{T}^2$ $\hat{\rho}^2(\theta_{gs}^\circ - 1) C_{pl}/C_{pg}$
$t_e$ evaporation time (time for $R_1$ to decrease to 0.05) [s]
$u$ velocity [cm s$^{-1}$]
$u_e$ velocity associated with the gases evolved through evaporation [cm s$^{-1}$]
$u_r$ relative velocity, $(u_\infty - u_c)$ [cm s$^{-1}$]
$u_\infty$ far field flow velocity [cm s$^{-1}$]
$V_d$ $4\pi R^3/3$ [cm$^3$]
$\hat{V}_1$ $(4\pi n R^{\circ 3})^{-1} - R_2^3/3$
$\hat{V}_2$ $(4\pi n R^{\circ 3})^{-1} - R_1^3/3$
$V_T$ $\mathscr{V}/N$
$\mathscr{V}$ $4\pi\tilde{R}^3/3$ [cm$^3$]
$W_i$ molecular weight of species $i$ [g mol$^{-1}$]
$\hat{Y}_F$ $\int_{R_1}^{R_2} Y_{Fv}^\circ(y) y^2 \, dy + \hat{V}_1 Y_{Fva}^\circ$
$Y_i$ mass fraction of species $i$
$y$ $r/R^\circ$
$z$ $r/R$.

Greek symbols

$\alpha$ constant
$\Delta C_p$ fitted $C_{pl}$–$C_{pg}$ for the saturation pressure curve [cal g$^{-1}$ K$^{-1}$]
$\xi$ $-2 \ln R_1(t)$
$\varepsilon_V$ $V_d/V_T$
$\theta$ $C_p T/L_{bn}$
$\lambda$ conductivity [cal cm$^{-1}$ s$^{-1}$ K$^{-1}$]
$\tau$ defined by equation (5)
$\sigma$ $-\rho_l C_{pl} R(dR/dt)/\lambda_l$
$\phi$ air/fuel mass ratio
$\phi_s$ stoichiometric air/fuel mass ratio
$\rho$ density [g cm$^{-3}$]
$\hat{\rho}$ $\rho/\rho_{ga}^\circ$
$\hat{\rho}^1$ $(R_2^3 - 1)/3 + \hat{V}_1$
$\hat{\rho}^2$ $\hat{\rho}_1^\circ/3$
$\nu$ kinematic viscosity [cm$^2$ s$^{-1}$]
$\chi$ defined by equation (21)
$\Psi$ equivalence ratio, $\phi/\phi_s$.

Subscripts

a at the edge of the sphere of influence
ag ambient gas
bn normal boiling point
c cluster
d droplet
F fuel
g gas
l liquid
0 initial
p partial
s droplet surface
sat saturation
st stagnation
v vapor.

Superscripts

° initial.

The results obtained by solving this system of equations are discussed in Section 4, and finally in Section 5 the main features of the model are recalled and conclusions are presented. All the symbols used are identified in the Nomenclature.

## 2. MODEL FORMULATION

Figure 1 shows the physical picture studied here. A moving spherical cluster of monodisperse, uniformly distributed, spherical droplets made of single-com-

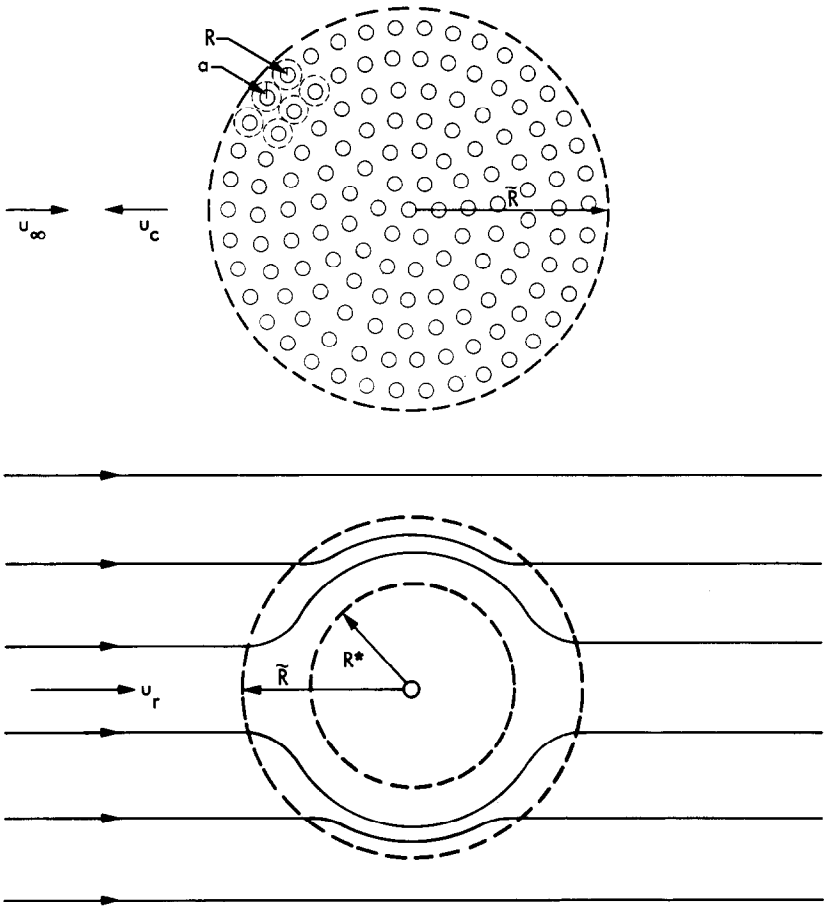


FIG. 1. Physical picture of the cluster of drops in a convective flow. (a) System of coordinates attached with the ambient gas. (b) System of coordinates attached with the cluster.

ponent fuel depicts a collection of drops from a spray that is exposed to a convective flow characterized by the velocity $\mathbf{u}_\infty$. A real spray is viewed here as a multitude of these clusters of drops, but the present formulation is restricted to the description of one individual cluster.

The droplets in the cluster are all assumed to move with the same velocity, $\mathbf{u}_c$. Thus, in the frame of reference attached to the center of the cluster, the velocity of the flow past the cloud is $\mathbf{u}_r = \mathbf{u}_\infty - \mathbf{u}_c$. The equations describing evaporation of the cluster are written in this frame of reference.

As in the model of Bellan and Cuffel [1], each droplet of the cluster is considered surrounded by a fictitious sphere of influence; the ensemble of these closely-packed spheres and the spaces between them is the entire volume of the cluster. The gas surrounding the droplets is typically air which might have been vitiated. Furthermore, it is assumed that: the gas phase is quasi-steady with respect to the liquid phase (reasonable for low pressure conditions); the drop temperature is a function of droplet radius and time (justified for very viscous liquids, such as heavy fuel oils, where recirculation of the flow inside the drop is minimal and the limit of zero Hill vortex strength is applicable [2]); the temperature is a continuous function at the drop surface; all dependent variables are averaged in the spaces between the spheres of influence; the Lewis number of the gas phase is unity; the quantity $\rho D$ is constant; $C_{pg}$, $C_{pl}$, $\lambda_g$ and $\lambda_l$ are averaged and constant; $\rho_g$ is time dependent but uniform; $\rho_l$ is constant; the cluster is not exposed to body forces; the Mach number of the gas phase is much smaller than unity; radiative and other heat-loss mechanisms are neglected.

For reasons explained below we adopt the classical approach [3, 4] that does not attempt the detailed prediction of the flow field around each drop when a cluster is exposed to a convective flow. Instead, what is of interest here is the modification of the value of the evaporation rate due to the convective flow as well as global features of the ensemble of drops. For this reason, we will still use here a model of quiescent evaporation and the modification of the evaporation rate will be described according to well-known correlations [4].

### A. *The liquid-phase formulation*

The life history of a droplet of single-component

fuel is described entirely by the energy equation

$$4\pi r^2\rho_l C_{pl}\frac{\partial T_l}{\partial t}-\frac{\partial}{\partial r}\left(4\pi r^2\lambda_l\frac{\partial T_l}{\partial r}\right)=0. \quad (1)$$

The appropriate boundary conditions are

$$\left.\frac{\partial T_l}{\partial r}\right)_{r=0}=0 \quad (2)$$

$$\left.-4\pi R^2\lambda_l\frac{\partial T_l}{\partial r}\right)_{r=R}=\left.-4\pi R^2\lambda_g\frac{dT_g}{dr}\right)_{r=R}+\dot{m}L. \quad (3)$$

In order to simplify the numerical solution technique, equations (1)–(3) are solved in a system of coordinates fixed with the regressing droplet surface. These new coordinates $(z,\tau)$ are introduced as follows:

$$z=\frac{r}{R(t)} \quad (4)$$

$$\tau=\frac{t}{\tilde{\beta}},\quad \tilde{\beta}=C_{pg}\frac{\rho_l^\circ R^{\circ 2}}{\lambda_l}. \quad (5)$$

Once nondimensionalized and transformed into this new system of coordinates, equations (1)–(3) become

$$z^2\frac{\partial\theta_l}{\partial\tau}-\left(z^3\frac{C}{R_l^3}\frac{\lambda_g}{\lambda_l}+2z\frac{1}{R_l^2}\frac{C_{pg}}{C_{pl}}\right)\frac{\partial\theta_l}{\partial z}-\frac{z^2}{R_l^2}\frac{C_{pg}}{C_{pl}}\frac{\partial^2\theta_l}{\partial z^2}=0 \quad (6)$$

$$\left.\frac{\partial\theta_l}{\partial z}\right)_{z=0}=0 \quad (7)$$

$$\left.\frac{\partial\theta_l}{\partial z}\right)_{z=1}=R_l\frac{\lambda_g}{\lambda_l}\left.\frac{d\theta_g}{dy}\right)_{y=R_l}+\frac{C}{R_l}\frac{\lambda_g}{\lambda_l}\frac{L}{L_{bn}} \quad (8)$$

$C$ is here a nondimensional evaporation rate as defined in the Nomenclature.

B. *The kinetic evaporation law*

Evaporation of a substance at a surface is the result of the difference between the flux of molecules of the substance leaving the surface and that of molecules of the same substance striking the surface [5]. This is expressed by:

$$\dot{m}=\alpha R^2(p_{sat,s}-p_{p,s})\left(\frac{W_F}{2\pi\hat{R}_u T_{gs}}\right)^{1/2} \quad (9)$$

where

$$p_{sat,s}=(1\text{ atm})\exp\left[\frac{L_{bn}W_F}{R_u}\left(\frac{1}{T_{bn}}-\frac{1}{T_{gs}}\right)+\frac{\Delta C_p W_F}{R_u}\left(1-\frac{T_{bn}}{T_{gs}}+\ln\frac{T_{bn}}{T_{gs}}\right)\right] \quad (10)$$

$$p_{p,s}=\frac{Y_{Fvs}}{W_F}\frac{1}{\sum_i Y_i/W_i}p_s. \quad (11)$$

In equation (10) we made the implicit assumptions that the gas is perfect, away from the critical point, and that $\Delta C_p$ is a constant.

When nondimensionalized, the kinetic evaporation rate equation becomes

$$C=-\alpha R_l^2\frac{R^\circ}{4\pi\rho_g D}\left\{(1\text{ atm})\exp\left[\frac{C_{pg}W_F}{R_u}\left(\frac{1}{\theta_{bn}}-\frac{1}{\theta_{gs}}\right)+\frac{\Delta C_p W_F}{R_u}\left(1-\frac{\theta_{bn}}{\theta_{gs}}+\ln\frac{\theta_{bn}}{\theta_{gs}}\right)\right]-\frac{Y_{Fvs}}{W_F}p_s\Big/\left[Y_{Fvs}\left(\frac{1}{W_F}-\frac{1}{W_{ag}}\right)+\frac{1}{W_{ag}}\right]\right\}\times\left(\frac{W_F C_{pg}}{2\pi\hat{R}_u L_{bn}}\frac{1}{\theta_{gs}}\right)^{1/2}. \quad (12)$$

Equation (12) is the correct form of the evaporation law which is often simplified to yield the Clausius–Clapeyron relationship. That relationship has been extensively used despite the fact that it has been shown to lead sometimes to inconsistencies and inaccuracies [5].

C. *The gas-phase formulation*

The set of equations describing the behavior of the mass fractions, temperature, density and pressure during evaporation in quiescent surroundings has been developed in ref. [1]. To summarize it, two sets of equations were formulated. The first set described evaporation of an individual droplet inside its own sphere of influence. The second set were global conservation equations inside the control volume of the cluster and they described the behavior of the dependent variables at the edge of the sphere of influence. Thus they were coupled to the first set of equations. The Appendix contains the solution of this set of equations in terms of the dependent variables. This solution is still valid here with the exception of the calculation of the evaporation rate, $C$, which is now different due to the existence of the convective flow. The model used for calculating $C$ is described next.

Sprays exposed to convective flows behave very differently from quiescent clouds of drops. First, the geometry of the entity changes due to turbulence-induced flows and recirculation. Second, the evaporation rate increases. Both the change in geometry and the enhancement of evaporation are very difficult to model; the main concern here is the determination of the evaporation rate. It has been established long ago [3] that when an individual drop is exposed to a flow past it, its evaporation rate increases and the new evaporation rate can be expressed in terms of the evaporation rate in quiescent surroundings multiplied by a factor containing the Reynolds number. More recently, Prakash and Sirignano [2] and Dwyer and Sanders [6] have modeled the details of the external flow around a droplet and the coupled internal flow dynamics inside the droplet for a droplet immersed

in a convective flow. However, these results are not directly applicable to drops in a nondilute spray because the flow around each drop of the spray is influenced by the presence of the other drops. Tal *et al.* [7] have mathematically treated the situation of flow over three equal and constant-diameter spheres equally spaced in one direction and found that a remarkable hydrodynamic periodicity evolved beginning with the first sphere after the inlet-exposed sphere. In fact, both the drag coefficient and the Nusselt number tend to stabilize after the second sphere. In contrast, the temperature field was found aperiodic and had to be resolved for each particular sphere. It is difficult to predict how these results might change when evaporation and the resulting decrease in sphere-size are considered.

It is obvious that when describing a nondilute cluster composed of a multitude of droplets it is impractical to attempt a detailed description of the exterior and interior flow patterns, temperature and mass fractions around and inside each drop, unless there is indeed a common aspect to all of them. Therefore, one needs to reconsider the interactions between a cluster and the surrounding flow so as to isolate the important and relevant aspects. These are taken to be as follows: (i) extent of the flow penetration inside the cluster volume at each instant in order to assess which droplets are aware of the existence of the flow; (ii) the magnitude of the instantaneous relative velocity between the cluster and the flow; and (iii) the relationship between the evaporation rate with and without flow.

To assess whether the interior of the cluster is penetrated by the outer flow, a comparison between the flow of gases yielded by evaporation from the drops and the flow of gases coming from the outer flow at the cluster surface is made here. This yields a dynamic criterion for cluster penetration similar to a static criterion previously developed [8]. Based upon the results of previous calculations [1], the pressure inside the cluster is considered equal to that in the ambient flow. Then, at instant $t$, the cluster will not be penetrated if

$$\rho_{ga}^{\circ} u_r^2 < \rho_{g,c} u_e^2. \tag{13}$$

But

$$u_e = \dot{M}/\rho_{g,c} \tag{14}$$

$$\dot{M} = \dot{m} n \mathscr{V}/\mathscr{S} = \dot{m} n \tilde{R}/3 \tag{15}$$

so that the criterion becomes

$$\dot{m} > 3 \frac{u_r}{n\tilde{R}} \sqrt{\rho_{ga}^{\circ} \rho_{g,c}}. \tag{16}$$

Nondimensionalizing, identifying $\rho_{g,c}$ as $\rho_{ga}$ and defining $C^*$ as

$$C^* = \frac{3}{4\pi} \frac{1}{\tilde{R}R^{\circ}} \frac{u_r \rho_{ga}^{\circ}}{n(\rho_g D)} \sqrt{\hat{\rho}_{ga}} \tag{17}$$

the criterion specifies that no flow penetration will occur for

$$|C| > C^*. \tag{18}$$

Since $C^*$ is directly proportional to $u_r$, this is an additional reason for calculating $u_r$ as a function of $t$. This is done here by solving the momentum equation for a sphere moving through a fluid:

$$m_c \frac{d\mathbf{u}_c}{dt} = -\frac{\pi}{8} d_c^2 \rho_g C_D |\mathbf{u}_c - \mathbf{u}_\infty| (\mathbf{u}_c - \mathbf{u}_\infty). \tag{19}$$

If complete penetration of the flow occurs, the sphere is each individual droplet; however, if there is no penetration by the outer flow, the sphere is the entire cluster because the flow goes past the cluster. In order to have a smooth transition between these two extremes, partial penetration is considered as well. For this purpose, an effective radius of the sphere is defined as

$$R^* = R + (\tilde{R} - R) \min(1, \sqrt{\chi}) \tag{20}$$

where

$$\chi = \frac{|C|}{C^*} = \frac{u_c}{u_\infty - u_c}. \tag{21}$$

With this formulation, if $|C| > C^*$, there is no penetration and $R^* = \tilde{R}$, as expected. If $|C| \leqslant C^*$ there is penetration and $R^* = R_{st}$ where $R_{st}$ is the equivalent radius of the stagnation point surface for the solution of the incompressible potential flow around a sphere. The $\sqrt{\chi}$, rather than $\chi$, was chosen in the definition of $R^*$ in order to introduce the similarity with the incompressible potential flow solution for the stagnation point. When $|C| \ll C^*$ there is complete penetration and $R^* = R$, as expected. In equation (19)

$$d_c = 2R^* \tag{22}$$

and

$$m_c = \frac{4\pi}{3} \rho_c R^{*3} \tag{23}$$

$$\rho_c = \frac{m_d + m_g}{V_T} = \rho_l \varepsilon_v + \rho_g (1 - \varepsilon_v). \tag{24}$$

In this manner, all possibilities are described by the general momentum equation

$$\frac{du_r}{dt} = -\frac{3}{8} \frac{\rho_g}{\rho_c} \frac{1}{R^*} C_D u_r^2 \tag{25}$$

where

$$C_D = 0.271 Re^{0.21} \tag{26}$$

$$Re = \frac{2R^* u_r}{\nu_{ag}}. \tag{27}$$

Equation (26) represents a correlation valid for Reynolds number up to $10^4$ [4, 9]. Reliable correlations for higher Reynolds numbers have not been found. If such relations become available, they can easily be incorporated into this model.

When a cluster is not penetrated by the flow around

it, a distinction must be made between the drops of the outer shell whose evaporation is affected by the flow and the inner drops whose evaporation is not affected by it. Thus the average evaporation rate of the cluster is defined as

$$C = C_{Re}\left(\frac{R^*}{\tilde{R}}\right)^3 + C_{Re}\left[\left(\frac{R^*}{\tilde{R}}\right)^3 - \left(\frac{R^*-a}{\tilde{R}}\right)^3\right] + C_{Re}\left(1-\frac{R^*}{\tilde{R}}\right)^3 \quad (28)$$

where

$$C_{Re_i} = C_{(Re=0)}\left[1 + \frac{0.278 Re_i^{0.5}}{(1+1.237/Re_i)^{0.5}}\right] \quad (29)$$

and

$$Re_1 = 0 \quad (30)$$

$$Re_2 = Re \quad (31)$$

$$Re_3 = \frac{2Ru_r}{\nu_{ag}}. \quad (32)$$

In equation (28) the first term on the RHS accounts for the evaporation of the drops in the core of the cluster, the second term represents the evaporation of the droplets in the outermost shell of the sphere of radius $R^*$, whereas the third term accounts for the evaporation of the drops in the spherical shell between the radius $R^*$ and $\tilde{R}$, as shown in Fig. 1. The correlation for $C_{Re_i}$ was used extensively [4] and reduces to the Ranz–Marshall expression in the limit of very large Reynolds numbers. As it will be pointed out in the discussion of the results, the effective radius $R^*$ as defined by equation (20) is a good representation for dense clusters but becomes less appropriate as the cluster becomes more dilute.

## 3. NUMERICAL PROCEDURES

One of the complications in making calculations with the present model, as compared to the previously mentioned one [1], is that the drop temperature distribution must be found at each time step. Another complication is that the kinetic evaporation law, along with the equation of state, form a nonlinear implicit set of equations for the pressure and evaporation rate, $C$, if $\theta_{gs} = \theta_{ls}$ is assumed. These equations must be numerically iterated to solve for the pressure and evaporation rate.

In order to treat the drop temperature distribution equation, the independent variable is changed from time to a new time-like variable:

$$\xi(t) \equiv -2\ln R_1(t). \quad (33)$$

The drop heat conduction equation becomes

$$\sigma(\xi)\,2\frac{\partial\theta_1}{\partial\xi} + z\frac{\partial\theta_1}{\partial z} = \frac{\partial^2\theta_1}{\partial z^2} + \frac{2}{z}\frac{\partial\theta_1}{\partial z} \quad (34)$$

where

$$\sigma \equiv -\frac{\rho_l C_{pl}}{\lambda_l} R\frac{dR}{dt}. \quad (35)$$

The surface boundary condition may be written as

$$\frac{\partial\theta_1}{\partial z} = -\sigma(\xi)G(\xi) \quad \text{at } z = 1 \quad (36)$$

where the function $G$ depends on the surface temperature, normalized radius $R_1$, and evaporation parameter, $C$. (The total dependence on the surface temperature is highly nonlinear. This poses potential numerical stability problems.) The function $\sigma$ is relatively small for cases of interest and is very weakly varying. An expansion in parameter $\sigma$ may be made; it was found that this is equivalent to expanding $\theta_1$ in powers of $z^2$. (Odd powers do not appear due to radial symmetry.) A four-term truncated series, to order $(z^6)$, gives adequate numerical accuracy. Let

$$\theta_1 = \sum_{j=0}^{3} B_j(\xi) z^{2j}, \quad \text{with } \theta_{ls} \equiv \theta_1\ (z=1).$$

Then in terms of $\theta_{ls}$ and a function $F(\xi)$

$$B_0 = \theta_{ls} + \frac{35}{8}\left(1-\frac{2}{63}\sigma\right)F - \frac{3}{8}\left(1-\frac{2}{27}\sigma\right)\sigma G$$

$$B_1 = \frac{5}{4}\left(1-\frac{1}{9}\sigma\right)\sigma G - \frac{35}{4}\left(1-\frac{5}{63}\sigma\right)F$$

$$B_2 = \frac{7}{8}\left(1-\frac{2}{9}\sigma\right)(5F-\sigma G)$$

$$B_3 = \frac{1}{12}\sigma(5F-\sigma G)$$

where

$$F = \left(1-\frac{5}{63}\sigma\right)w(\xi) + \frac{2}{63}\sigma\frac{dw}{d\xi}$$

$$\frac{d}{d\xi}(\theta_{ls}+F) = -\frac{3}{2}(G-F)$$

$$\frac{4}{45}\sigma\frac{dw}{d\xi} + \left(1-\frac{1}{45}\sigma\right)w = \frac{1}{5}\sigma G.$$

These give a consistent solution, accurate to order $(\sigma^3)$, in terms of the two unknown functions $(\theta_{ls}+F)$ and $w$.

The numerical integration is carried out using the GEAR integrator package [10]. For each integrator step, the following iterative procedure is applied.

(i) Predict values of $F$, $G$, $\theta_{ls}$.
(ii) Solve the equation of state and the kinetic evaporation law by Newton–Raphson iteration for the pressure and evaporation rate.
(iii) Apply the convection correction to the evaporation rate.
(iv) Correct the values of $F$, $G$, $\theta_{ls}$.

A repeat is made starting at (ii) until convergence is obtained. Thus, each step requires a double-loop iteration to calculate the surface temperature, evaporation rate, and pressure.

## 4. DISCUSSION OF RESULTS

One of the goals of the present research is to develop a self-consistent model of convective spray evaporation that will qualitatively agree with experimental observations. For this reason we are interested in the extent of the external flow penetration inside the cluster and how this penetration influences evaporation. We are also interested to determine to what extent the temperature profile inside each drop of the cluster becomes nonuniform during heating and evaporation, and finally we want to identify the parameters most critically affecting the evaporation.

All calculations here were performed for drops of initial radius $R^\circ = 2 \times 10^{-3}$ cm using $n$-decane as the fuel and air as the ambient gas. Table 1 illustrates various thermophysical constants used in the calculations and Table 2 shows the actual parameters that were varied during the calculations and the range within which they varied. In general, calculations were performed for a rich cluster and a high ambient temperature so as to simulate evaporation of a dense cluster of drops immersed in a hot environment resulting from combustion of other clusters previously injected.

Table 1. Parameters and thermophysical properties used in the calculations

| | |
|---|---|
| $\tilde{R} = 10$ cm | |
| Gas phase: | $W_F = 142$ g mol$^{-1}$ |
| | $W_{ag} = 28.9$ g mol$^{-1}$ |
| | $C_{pg} = 0.241$ cal g$^{-1}$K$^{-1}$ |
| | $D^\circ = 0.1$ cm$^2$ s$^{-1}$ |
| Liquid phase: | $\rho_l = 0.734$ g cm$^{-3}$ |
| | $C_{pl} = 0.523$ cal g$^{-1}$ K$^{-1}$ |
| | $\lambda_l = 2.5 \times 10^{-4}$ cal g$^{-1}$ K$^{-1}$ |
| | $\mu_l = 1.35 \times 10^{-2}$ g cm$^{-1}$ s$^{-1}$ |
| | $T_{bn} = 447.7$ K |
| | $L_{bn} = 73.92$ cal g$^{-1}$ |

Table 2. Values of the parameters used in the parametric study

| $\Psi$ | $u_r^\circ$ (cm s$^{-1}$) | $T_{ga}^\circ$ (K) | $T_{gs}^\circ$ (K) | $Y_{Fva}^\circ$ |
|---|---|---|---|---|
| 0.02 | sweep | 2000 | 350 | 0.0 |
| sweep | 200 | 2000 | 350 | 0.0 |
| sweep | 1000 | 2000 | 350 | 0.0 |
| 0.02 | 1000 | sweep | 350 | 0.0 |
| 0.02 | 1000 | 2000 | sweep | 0.0 |
| 0.02 | 1000 | 2000 | 350 | sweep |

| Sweeps: | |
|---|---|
| $\Psi$ | (0.005), 0.02, 0.05, 0.10, 0.20, 1.00, 5.00, 10.00, 20.00, 50.00 |
| $u_r^\circ$ (cm s$^{-1}$) | 10, 25, 50, 100, 300, 750, 1500, 2000 |
| $T_{ga}^\circ$ (K) | 750, 1000, 1500, 2000, 2500 |
| $T_{gs}^\circ$ (K) | 350, 380, 410, 440 |
| $Y_{Fva}^\circ$ | 0.00, 0.01, 0.05, 0.06, 0.07, 0.10, 0.15, 0.155. |

The plot in Fig. 2 shows that there are three regions where the evaporation time exhibits different behaviors. The first region is that of very dense clusters where evaporation is hindered by accumulation of fuel vapor in the gas phase so that eventually saturation is obtained before complete evaporation. In contrast to the other regions, here the evaporation time is defined as the time when evaporation stops so that as $\phi$ increases saturation is obtained faster and thus $t_e$ decreases. The second region is that of dense clusters where evaporation is enhanced as the cluster becomes more dilute because there is more coupling between the gases and the drops as the cluster becomes more penetrated by the gases. The third region is that of the

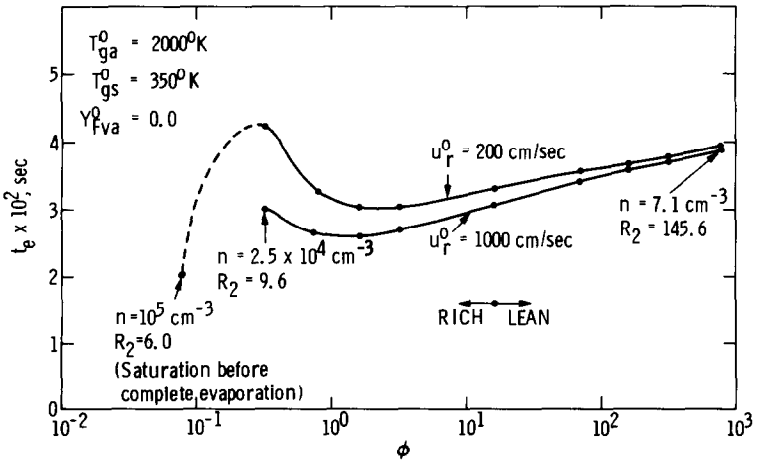


FIG. 2. Evaporation time versus the mixture ratio for two initial relative velocities between the cluster and the gases.

dilute and very dilute clusters where it is predicted that the evaporation time increases as the cluster becomes more dilute. These last results are questionable and must await further confirmation since as it will be shown below the model becomes invalid at large penetration distances. For the same mixture ratio, a larger initial relative velocity will accelerate evaporation, as expected. (It should be pointed out that the cases of the very dilute clusters exposed to a large initial relative velocity might be somewhat unrealistic since it is difficult to imagine that a cluster containing so little mass can sustain significant relative velocities.)

The above results are qualitatively correct with the understanding that the predictive ability of the model deteriorates as the cluster is more dilute or becomes more penetrated by the outer flow. This can be seen in Fig. 3 where a nondimensional expression related to the penetration is plotted vs $R_1$. For very dense clusters there is initially little or no penetration, but as evaporation proceeds $u_e$ decreases faster than $u_r$ and so penetration becomes more important. When the cluster is substantially penetrated, the present model becomes invalid because for this condition the Reynolds number should be based upon another length than the penetration distance as defined in equation (20). The same comment is valid for the characteristic distances included in the definitions of equations (22)–(24). Since the solution of the momentum equation is a function of these definitions, it is expected that the prediction of the relative velocity as a function of time is also somewhat in error. The choice of the appropriate characteristic distance to be used in this relationship is not obvious and additional modeling is needed to remove this difficulty. Since for dense or dilute clusters the penetration distance seems non-negligible the development of a more accurate model seems necessary. It is however expected that the trends presented here are still correct, although for example the slope of the curves presented in Fig. 2 will change. In order to compare the present results with the classical single-droplet-in-quiescent-environment solution we display in Fig. 4 a plot of $R_1^2$ vs time for various values of $\Psi$. As expected, none of these curves is a straight line, except in the one case where the cluster is so dense as to lead to saturation before complete evaporation.

To ensure that our results are as correct as possible, the next parametric studies were all made for rather dense clusters where the convective evaporation model performs best.

Figure 5 shows the influence of $u_r^\circ$ upon the evaporation time of the cluster. The important observation here is that the evaporation time seems to be only a weak function of $u_r^\circ$. For example, increasing $u_r^\circ$ by a factor of 10 from 10 to 100 cm s$^{-1}$ decreases $t_e$ by only 26% and increasing $u_r^\circ$ by a further factor of 20 to 2000 cm s$^{-1}$ decreases $t_e$ by only 45%. The practical conclusion is that for clusters, as distinct from isolated drops, large increases in the initial relative velocity must be planned before significant reductions in the evaporation time can be expected.

In contrast, the results of Fig. 6 show that, in the lower temperature regime, the initial ambient temperature plays an important role in controlling the evaporation time of the cluster. Beyond 1500 K, little

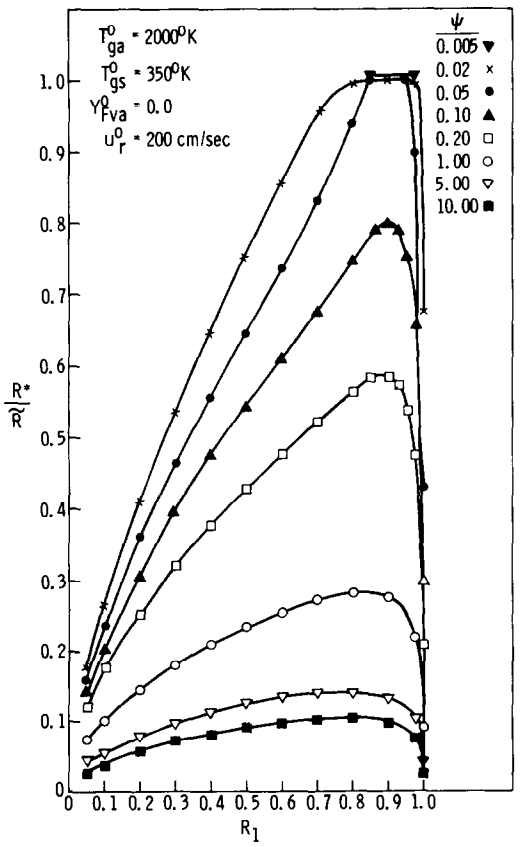


FIG. 3. Normalized residual penetration distance vs normalized instantaneous droplet radius for various equivalence ratios (rich: $\Psi < 1$; lean: $\Psi > 1$). The penetration distance is defined as $\tilde{R}(1-R^*/\tilde{R})$.

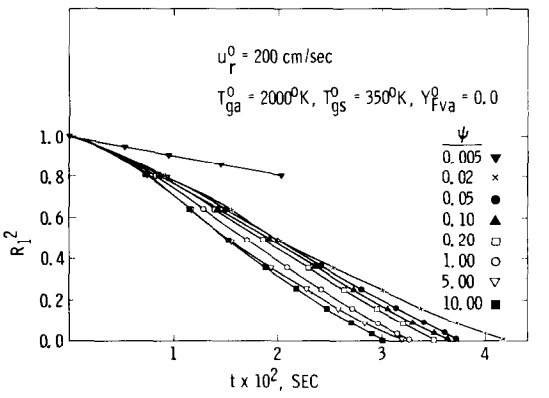


FIG. 4. Variation of the normalized square radius with time for various equivalence ratios (rich: $\Psi < 1$; lean: $\Psi > 1$).

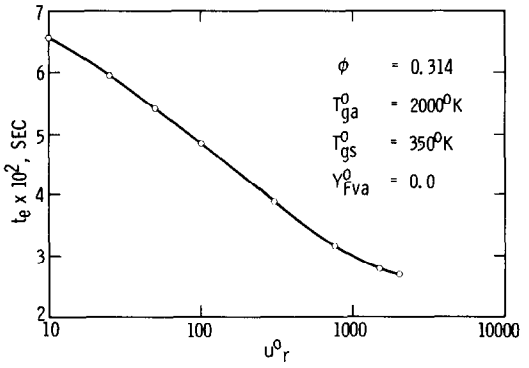


FIG. 5. Evaporation time vs the initial relative velocity between the cluster and the gas.

is gained by further increasing the initial temperature of the surrounding gases. The results obtained by varying $T^\circ_{ga}$ were also used to study the drop-temperature nonuniformities during evaporation. This is because the variation of $T^\circ_{ga} - T^\circ_{gs}$ allowed the observation of steeper gradients developing as this temperature difference increased. Plotted in Fig. 7 is the time-history of the nondimensional drop temperature vs the nondimensional drop radius for the largest difference $T^\circ_{ga} - T^\circ_{gs}$ where most nonuniformities developed. Initially, the drops are introduced at constant temperature but very quickly a gradient develops due to the heat demanded for evaporation. [This is to say that in the very initial period, the boundary condition expressed by equation (3) controls the dynamics of evaporation.] Simultaneously, the ambient temperature decreases substantially because heat is transported to the drop's surface to promote evaporation. It is to be noticed that by the time $R_l = 0.8$ the ambient temperature has decreased by factor of 2.2. This is explained by the fact that when $R_l = 0.8$, 49% of the drop's mass has already evaporated. The results presented in Fig. 7 also show that by the time

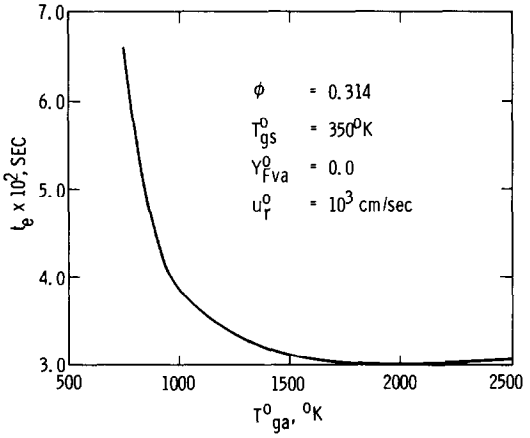


FIG. 6. Evaporation time vs the initial surrounding gas temperature.

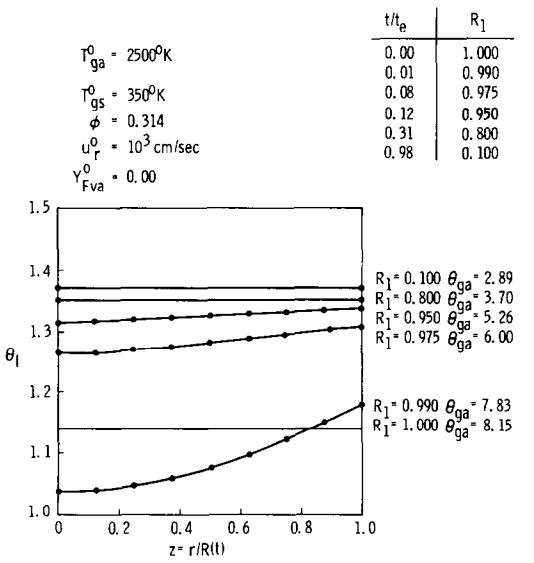


FIG. 7. Nondimensional internal drop temperature profile at various residual drop sizes.

$R_l$ has reached 0.8 the internal temperature profile has become uniform. In terms of time spent in a nonuniform temperature configuration, the drop has spent a third of its lifetime in this mode. Thus, according to the table in Fig. 7, two thirds of the droplet lifetime will be spent in a uniform temperature configuration during which about 50% of its mass will be evaporated. These results are in partial disagreement with those obtained by Prakash and Sirignano [2] for individual single-component fuel drops for which drop-temperature nonuniformities persisted up to the end of the drop's life. It is unclear at this point if this is due to their more sophisticated interior-droplet model or to the fact that they study only individual drops. The viscosity of the fuel here is large enough to make the zero-Hill-vortex-strength limit acceptable and thus the present model seems appropriate. In fact, a calculation of the ratio of the characteristic time for circulation to the characteristic time for heat-up, $[(\lambda_l/\rho_l C_{pl})]/(\mu_l/\rho_l)$ shows that this ratio is $3.53 \times 10^{-2}$ (the values of the constants are given in Table 1), and thus the heating time is indeed independent of the circulation time which makes the model and the results self-consistent. In agreement with ref. [2] we found that unsteadiness in the liquid phase persisted to the end of the drop's lifetime.

The strong dependence of $t_e$ upon $T^\circ_{gs}$ is shown in Fig. 8, where it is seen that about 20% increase in the initial drop temperature results in about 34% decreases in the evaporation time. For an initial temperature close to the normal boiling point the drops are initially so hot that evaporative cooling is observed up to $R_l = 0.8$ (23% of the droplet lifetime) after which heating occurs again.

Figure 9 shows that $t_e$ has a very weak dependence upon $Y^\circ_{Fva}$ for rich mixtures, merely because the drop number density changes very slowly with $Y^\circ_{Fva}$. For

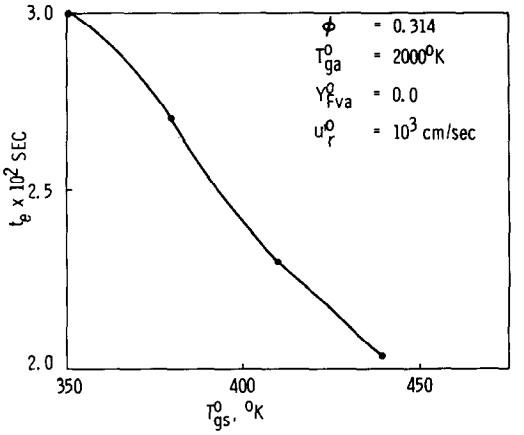


FIG. 8. Evaporation time vs the initial drop temperature.

these rich mixtures $Y^{\circ}_{Fva}$ can be increased as much as to obtain saturation at the initial condition and it is found that in the entire regime $t_e$ depends linearly upon $Y^{\circ}_{Fva}$.

## 5. SUMMARY AND CONCLUSIONS

The model of convective droplet-cluster evaporation developed herein is based upon the concept of a penetration distance defined as the distance that the outer flow penetrates into the cluster volume. If there is no penetration, the outer flow bypasses the cluster of drops and only the drops at the periphery of the cluster feel the effect of the convective flow. If the flow penetrates completely, each drop feels the effect of this outer flow. Partial penetration was also considered, and included in this model is an expression developed by similarity with the incompressible potential flow around a sphere. In all situations, the decrease in the relative velocity between the cluster and the gases was calculated using a momentum equation for the cluster that takes drag into account. The evaporation enhancement due to the convective flow was modeled using a correlation based upon the Reynolds number.

Results obtained with this model show that the theory is valid for very dense and dense clusters when the penetration distance is small. As the penetration distance increases, the model is no longer self-consistent and additional considerations must be raised to find an alternate to the definition of the penetration distance as done here. However, the trends of the results are still expected to be correct especially since most of the situations considered here were those of dense clusters in hot environments.

Parametric variations have shown that there are three regions where the evaporation time exhibits a different behavior. In the very dense cluster regime where saturation is obtained before complete evaporation, the evaporation time (defined here as the time when evaporation stops) decreases as the cluster becomes denser. In the dense cluster region where no saturation is encountered, the evaporation time decreases as the cluster becomes more dilute. Finally in the dilute and very dilute regimes the evaporation time increases as the cluster becomes more dilute. These last results must await further confirmation since the predictive ability of the model is questionable in these regimes. For the same equivalence ratio, the dependence of the evaporation time (defined as the time to reach $R_1 = 0.05$) upon $u^{\circ}_r$ was found to be weak over the range 10–2000 cm $s^{-1}$. In contrast, for ambient temperatures in the range 750–1500 K, the evaporation time was found to be a strong function of $T^{\circ}_{ga}$, whereas further increase in the temperature of the surroundings proved fruitless in decreasing the evaporation time. The initial drop temperature was shown to strongly affect evaporation, and close to the normal boiling point evaporative cooling was observed. For dense clusters, the initial vitiation of the surrounding gases affected the evaporation very little except when saturation was obtained, and then no evaporation occurred.

In all situations encountered here the internal temperature of the drops exhibited an unsteady variation throughout the drop's lifetime. However, nonuniform temperature profiles were observed only during the initial part of the drop's lifetime; the largest nonuniformities persisted for a third of the drop's lifetime corresponding to about 50% of mass evaporated.

All the results presented here are qualitative and further modeling is needed to improve the predictive ability of this droplet-cluster model.

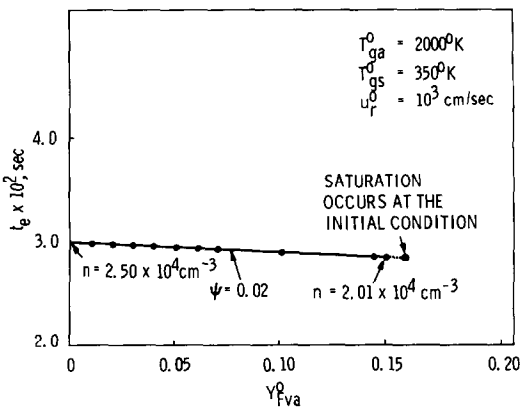


FIG. 9. Evaporation time vs the initial fuel vapor mass fraction at rich overall conditions.

*Acknowledgements*—This work was sponsored by the U.S. Department of Energy through an agreement with the National Aeronautics and Space Administration (DOE Interagency Agreement No. DE-A101-81CS66001: NASA Task No. RE-152, Amendment 308). The work was done for the Energy Conversion and Utilization Technologies Division, Mr Marvin Gunn, Jr, Program Manager, U.S. Department of Energy.

## REFERENCES


1. J. Bellan and R. Cuffel, A theory of non dilute spray evaporation based upon multiple drop interactions, *Combust. Flame* **51,** 55–67 (1983).
2. S. Prakash and W. A. Sirignano, Theory of convective droplet vaporization with unsteady heat transfer in the circulating liquid phase, *Int. J. Heat Mass Transfer* **23,** 253–268 (1980).
3. W. E. Ranz and W. R. Marshall, Evaporation from drops, *Chem. Engng Prog.* **48,** 141–173 (1952).
4. G. M. Faeth, Evaporation and combustion of sprays, *Prog. Energy Combust. Sci.* **9,** 1–76 (1983).
5. J. Bellan and M. Summerfield, Theoretical examination of assumptions commonly used for the gas phase surrounding a burning droplet, *Combust. Flame* **33,** 107–122 (1978).
6. H. A. Dwyer and B. R. Sanders, Detailed computation of unsteady droplet dynamics, Presented at the 20th Int. Symposium on Combustion (August 1984).
7. R. Tal, D. N. Lee and W. A. Sirignano, Hydrodynamics and heat transfer in sphere assemblages; multisphere cylindrical cell models, *Int. J. Heat Mass Transfer* **26,** 1265–1273 (1983).
8. J. Bellan and K. Harstad, Evaluation of the importance of slip velocity during evaporation of drops in sprays, Paper 84-1 presented at the Spring Meeting of the Western States Section/The Combustion Institute (1984). To be published in *Int. J. Heat Mass Transfer.*
9. F. Boysan, W. H. Ayers, J. Swithenbank and Z. Pan, Three dimensional model of spray combustion in gas turbine combustors, *J. Energy* **6,** 368–375 (1982).
10. A. C. Hindmarsh, GEAR : ordinary differential equation system solver, Lawrence Livermore Laboratory Report UCID-30001, Rev. 3 (December 1974).


## APPENDIX

The equations that yield the gas-phase solution are:

$$C = \frac{1}{R_2^{-1} - R_1^{-1}} \ln\left\{1 + (\theta_{ga} - \theta_{gs}) \Big/ \left[\frac{L}{L_{bn}} - \frac{R_1}{C}\frac{\lambda_l}{\lambda_g}\left(\frac{\partial \theta_l}{\partial z}\right)_{z=1}\right]\right\} \tag{A1}$$

$$Y_{Fvs} = (Y_{Fva} - 1)\,e^{C(R_1^{-1} - R_2^{-1})} + 1 \tag{A2}$$

$$R_1 = \left(1 + \frac{3\hat{\rho}_g D}{\hat{\rho}_l^{\circ} R^{\circ 2}} \int_0^t C\,dt\right)^{1/3} \tag{A3}$$

$$\varepsilon = 1 - R_1^3 \tag{A4}$$

$$\rho_{ga} = \frac{\hat{\rho}^{\,1} + \varepsilon \hat{\rho}^{\,2}}{f(R_1, R_2) + \hat{V}_1} \tag{A5}$$

$$Y_{Fva} = \frac{g(R_1, R_2, C)(\hat{Y}_F + \varepsilon\hat{\rho}^2) + Y_{Fvs}\rho_{ga}[e^{C/R_2} f(R_1, R_2) - I(R_1, R_2, C)]}{\hat{\rho}_{ga}[e^{C/R_1} f(R_1, R_2) - I(R_1, R_2, C) + \hat{V}_1 g(R_1, R_2, C)]} \tag{A6}$$

$$\begin{aligned}\theta_{ga} = \{ & g(R_1, R_2, C)[\hat{T}^1 + \hat{T}^2 - (\theta_{gs} - 1)\hat{\rho}^2 R_1^3 C_{pl}/C_{pg} \\ & + \hat{\rho}_{ga} f(R_1, R_2) + \hat{\rho}_{ga}\hat{V}_1] + \theta_{gs}\hat{\rho}_{ga}[e^{C/R_2} f(R_1, R_2) \\ & - I(R_1, R_2, C)]\} / \{\hat{\rho}_{ga}[e^{C/R_1} f(R_1, R_2) \\ & - I(R_1, R_2, C) + \hat{V}_1 g(R_1, R_2, C)]\}\end{aligned} \tag{A7}$$

$$\begin{aligned}p_{atm} = {} & R_u^*(L_{bm}/C_{pg})\rho_{ga}^{\circ}\frac{\hat{\rho}_{ga}}{\hat{V}_2}\left\{\left(\frac{1}{W_F} - \frac{1}{W_{ag}}\right)\frac{1}{[g(R_1, R_2, C)]^2}\right. \\ & \times [(Y_{Fva}\,e^{C/R_1} - Y_{Fvs}\,e^{C/R_2})(\theta_{ga}\,e^{C/R_1} \\ & - \theta_{gs}\,e^{C/R_2}) f(R_1, R_2) + [(Y_{Fva}\,e^{C/R_1} \\ & - Y_{Fvs}\,e^{C/R_2})(\theta_{gs} - \theta_{ga}) + (Y_{Fvs} - Y_{Fva}) \\ & \times (\theta_{ga}\,e^{C/R_1} - \theta_{gs}\,e^{C/R_2})] I(R_1, R_2, C) \\ & + (Y_{Fvs} - Y_{Fva})(\theta_{gs} - \theta_{ga}) I(R_1, R_2, 2C)] \\ & + \frac{1}{W_{ag}}\frac{1}{g(R_1, R_2, C)}[(\theta_{ga}\,e^{C/R_1} - \theta_{gs}\,e^{C/R_2}) \\ & \times f(R_1, R_2) + (\theta_{gs} - \theta_{ga}) I(R_1, R_2, C)] \\ & \left. + \alpha_p \hat{V}_1\left[Y_{Fva}\left(\frac{1}{W_F} - \frac{1}{W_{ag}}\right) + \frac{1}{W_{ag}}\right]\theta_{ga}\right\}.\end{aligned} \tag{A8}$$

## ANALYSE DE L'EVAPORATION CONVECTIVE D'ENSEMBLES DE GOUTTES NON DILUES


**Résumé**—On développe un modèle pour l'évaporation convective d'ensembles de gouttes. Le paramètre critique qui contrôle les différents modes d'évaporation a été identifié comme étant la distance de pénétration de l'écoulement externe dans le volume de l'ensemble. Un critère dynamique est développé pour distinguer la pénétration de la non pénétration. L'évaporation convective est modélisée à l'aide d'une formule à nombre de Reynolds entre le flux évaporé avec et sans convection. D'autres équations antérieurement développées [1] pour l'évaporation calme ont été utilisées ici, à l'exception d'une nouvelle loi cinétique d'évaporation à la surface de la gouttelette et d'un modèle de température interne non uniforme qui ont été introduits ensemble. Le modèle convient bien pour les faibles distances de pénétration qui correspondent aux clusters dense dans des environnements chauds et aux vitesses relativement faibles entre gaz et cluster. Pour ce cas, le modèle prédit que pour la même vitesse initiale le temps d'évaporation est plus court lorsque le cluster devient plus dilué. Pour des clusters dilués et des longueurs de pénétration grandes, on trouve le contraire. Puisque pour des grands longueurs de pénétration la valeur prédictive du modèle se détériore, ceci peut être mis en question. Néanmoins le temps d'évaporation est trouvé être une faible fonction de la vitesse relative initiale et une fonction forte de l'écart de température initial. La température initiale ambiante du gaz a une influence forte dans le régime des températures faibles 750–1500 K, tandis que l'influence est très faible au régime des températures fortes. La contamination du gaz ambiant par une vapeur combustible est trouvée avoir une très faible influence sur le temps d'évaporation pour des mélanges riches quand le cluster est introduit dans des environnements fortement convectifs à haute température. Dans tous les cas, les résultats montrent que la chute de température interne est variable pendant la durée de vie de la goutte, mais les non uniformités de la température persistent jusqu'à plus du premier tiers du temps total d'évaporation.

## ANALYSE DER KONVEKTIVEN VERDAMPFUNG VON UNVERDÜNNTEN TROPFENSCHWÄRMEN

**Zusammenfassung**—Ein Modell für die konvektive Verdampfung von unverdünnten Tropfenschwärmen wurde entwickelt. Als kritischer Parameter, der die verschiedenen Verdampfungsarten kontrolliert, wurde die Eindringtiefe der Außenströmung in das Schwarmvolumen identifiziert. Ein dynamisches Kriterium, das zwischen Eindringen und Nicht-Eindringen unterscheidet, wurde entwickelt. Die konvektive Verdampfung wurde dadurch modelliert, daß eine Reynolds-Zahl-Korrelation zwischen der Abdampfrate mit Konvektion und der Abdampfrate ohne Konvektion benutzt wurde. Andere Gleichungen, die bereits früher für ruhende unverdünnte Sprühverdampfung entwickelt wurden [1], wurden hier ebenso benutzt, mit der Ausnahme, daß ein neues kinetisches Verdampfungsgesetz für die Tropfenoberfläche und ein ungleichmäßiges inneres Temperaturmodell, welche hier entwickelt wurden, eingesetzt wurden. Es zeigte sich, daß das Modell für kleine Eindringtiefen, die für dichte Schwärme in heißer Umgebung und kleine Relativgeschwindigkeiten zwischen äußerem Gas und Schwarm beobachtet werden, gute Ergebnisse liefert. Für dichte Schwärme mit kleinen Eindringtiefen, erhält man aus den Modellrechnungen, daß bei der gleichen Anfangsgeschwindigkeit die Verdampfungszeit kürzer wird je verdünnter der Schwarm ist. Für verdünnte Schwärme und große Eindringtiefen wurde das Gegenteil festgestellt. Da sich die Zuverlässigkeit des Modelles für große Eindringtiefen verringert, sind die letzten Trends fragwürdig. Weiter wurde gefunden, daß die Verdampfungszeit nur schwach von der anfänglichen Relativgeschwindigkeit, dagegen stark von der Anfangstemperatur der Tropfen abhängt. Die Anfangstemperatur des umgebenden Gases hat im unteren Temperaturbereich (750–1500 K) einen starken Einfluß, im oberen Temperaturbereich war der Einfluß schwach. Die Verunreinigung des umgebenden Gases durch Kraftstoff-Dampf hat einen sehr geringen Einfluß auf die Verdampfungszeit für reiche Mischungen, wenn der Schwarm in eine stark konvektive Hochtemperaturumgebung gebracht wird. In allen Fällen zeigten die Ergebnisse, daß die innere Tropfentemperatur während des Tropfenlebens instationär war, daß aber Ungleichmäßigkeiten der Temperatur längstens bis ein Drittel der Gesamtverdampfungszeit erhalten blieben.

## АНАЛИЗ КОНВЕКТИВНОГО ИСПАРЕНИЯ ПЛОТНЫХ СКОПЛЕНИЙ КАПЕЛЬ

**Аннотация**—Разработана модель конвективного испарения плотных скоплений капель. Критический параметр, характеризующий различные режимы испарения, определен как расстояние проникновения внешнего потока в объем скопления. Получен динамический критерий для нахождения различий между случаем с проникновением и без него. Конвективное испарение моделировалось с использованием числа Рейнольдса, выражающего соотношение между интенсивностями испарения с конвекцией и без нее. Используются уравнения, выведенные ранее [1] для устойчивого распылительного испарения, а также новый закон для кинетики испарения на поверхности капли и модель неоднородной внешней температуры, предложенная в данной работе. Показано, что модель наиболее пригодна для малых расстояний проницаемости, которые получаются для плотных скоплений в горячей окружающей среде и для низких относительных скоростей между наружными газами и скоплением капель. Для плотных скоплений с малыми расстояниями проницаемости результаты модели показывают, что для одной и той же начальной скорости время испарения становится меньше, по мере того, как скопление капель становится более плотным. Для плотных скоплений и больших расстояний проницаемости наблюдалось обратное явление. Поскольку для больших расстояний проницаемости результаты расчетов получаются менее точными, последние закономерности являются спорными. Более того, найдено, что время испарения слабо зависит от начальной относительной скорости и сильно зависит от начального перепада температуры. Обнаружено, что начальная температура окружающего газа оказывает сильное влияние при низкотемпературном режиме в области температур 750–1500 К, в то время как при более высоких температурах это влияние очень мало. Найдено, что искажения, вносимые парами топлива, слабо влияют на время испарения в обогащенных смесях, когда скопления капель вводятся в высокотемпературный конвективный поток. Во всех случаях результаты показывают, что внутренний перепад температуры изменяется в течение времени жизни капли, а неоднородности температуры сохраняются в течение первой трети времени испарения.